EurJIC
European Journal of Inorganic Chemistry

A Journal of ChemPubSoc Europe

Accepted Article

Title: Synthesis and catalytic evaluation of phosphanylferrocene ligands with cationic guanidinium pendants and varied phosphane substituents

Authors: Ondrej Barta, Ivana Cisarova, Ewa Mieczynska, Anna M. Trzeciak, and Petr Stepnicka

To be cited as: *Eur. J. Inorg. Chem.* 10.1002/ejic.201901057

Link to VoR: http://dx.doi.org/10.1002/ejic.201901057

WILEY-VCH

FULL PAPER WILEY-VCH

Synthesis and catalytic evaluation of phosphanylferrocene ligands with cationic guanidinium pendants and varied phosphane substituents

Ondřej Bárta,[a] Ivana Císařová,[a] Ewa Mieczyńska,[b] Anna M. Trzeciak,[b] Petr Štěpnička[a]*

Abstract: This contribution expands the still narrow class of functional ferrocene phosphanes with polar cationic groups, focusing on the synthesis and catalytic use of a series of phosphanylferrocene ligands bearing positively charged guanidinium tags, [R_2PfcCH_2NHC(NH_2)$_2$]Cl (**3a-d**), where fc = ferrocene-1,1'-diyl, R = isopropyl (**a**), cyclohexyl (**b**), phenyl (**c**), and 2-furyl (**d**). To probe the influence of phosphane substituents, these compounds were studied as supporting ligands in Pd-catalysed Suzuki-Miyaura cross-coupling of acyl chlorides with arylboronic acids, in analogous coupling of aryl bromides with arylboronic acids, and in Rh-catalysed hydroformylation of 1-hexene using *trans*-[RhCl(CO)(R_2PfcCH_2NHC(NH_2)$_2$-κ*P*)$_2$]Cl_2 complexes (**4a-d**) as pre-catalysts. The outcome of the cross-coupling reactions strongly depended on the educts, and no ligand generated a universally applicable catalyst when combined with $Pd(OAc)_2$. In the hydroformylation reactions, the catalyst based on **4d** led to lower conversions than all others, which performed rather similarly. Overall, the phenyl-substituted phosphane **3c** emerged as a good compromise, giving rise to reasonably efficient and stable catalysts in most cases (except for Suzuki-Miyaura biaryl cross-couplings, wherein electron-rich alkylphosphanes performed better than **3c**).

Introduction

The highly polar and positively charged guanidinium moiety has been used to modify inherently hydrophobic phosphane molecules, in particular, to increase their affinity towards polar solvents and water.[1, 2] In catalysis, the guanidinium unit can further act as a structure-controlling moiety, which exploits its hydrogen-bonding ability to stabilise a specific structure (*e.g.*, the structure of a reaction intermediate) and to direct molecular parts or reaction partners to specific positions.[3] In the chemistry of ferrocene phosphanes,[4] however, the guanidine modifying group has been utilised only scarcely (see compounds **A** and **B** in Scheme 1).[5]

[a] O. Bárta, Dr. I. Císařová, Prof. Dr. P. Štěpnička
Department of Inorganic Chemistry
Faculty of Science, Charles University
Hlavova 2030, 128 40 Prague, Czech Republic
E-mail: petr.stepnicka@natur.cuni.cz
Homepage: http://www.natur.cuni.cz
[b] Dr. E. Mieczyńska, Prof. Dr. A. M. Trzeciak
Department of Inorganic Chemistry
Faculty of Chemistry, University of Wrocław
ul. F. Joliot-Curie 14, 50-383 Wrocław, Poland
Homepage: https://chem.uni.wroc.pl/pl/jednostka-organizacyjna/12
Supporting information for this article is given via a link at the end of the document.

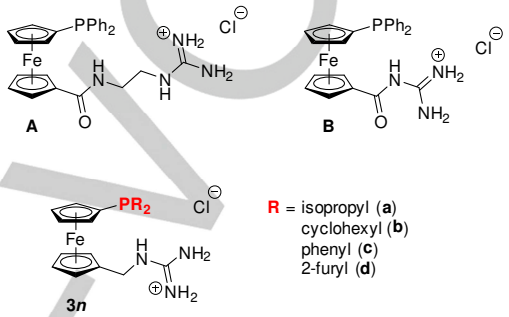

Scheme 1. Phosphinoferrocene ligands bearing guanidinium pendants. Note: among compounds **3**, only **3c** has been reported before.

Recently,[6] we have reported the facile synthesis of *N*-{[1'-(diphenylphosphanyl)ferrocene-1-yl]methyl}guanidinium hydrochloride (compound **3c** in Scheme 1) by guanylation[7] of [1'-(diphenylphosphanyl)ferrocene-1-yl]methylamine[8] and preliminary results from catalytic tests of this compound as an auxiliary ligand for Pd-catalysed cross-coupling reactions. To further develop the chemistry of phosphanylferrocene-guanidine ligands, we aimed to extend the series of such compounds by synthesizing analogues bearing *different* phosphane substituents, compounds **3** (Scheme 1). This contribution therefore describes the preparation of these functional phosphanes[9] and the results from a comparative catalytic study exploiting Pd-catalysed Suzuki-Miyaura cross-coupling[10] and Rh-catalysed hydroformylation[11] as benchmark reactions.

Results and Discussion

Ligand synthesis

The series of cationic phosphanylferrocene guanidine ligands **3** was expanded to include a pair of ligands with electronically and sterically similar electron-donating alkyl groups (R = *i*-Pr and Cy) and another pair of compounds with flat, conjugated, electron-withdrawing aryl groups at the phosphorus atom. Specifically, new guanidinium phosphanes **3a**, **3b** and **3d** were synthesized using a modified approach developed to prepare ligand **3c**.[6] In the first step, the starting phosphanylnitriles **1**[12] were reduced by Li[AlH_4] in THF to give the corresponding phosphanylamines **2** in practically quantitative yields. Subsequent reactions of the amines **2** with 1*H*-pyrazole-1-carboximidamide hydrochloride in the presence of triethylamine[13] produced phosphanyl-

guanidinium salts **3**, which were isolated in moderate to good yields by column chromatography, and subsequently crystallised. As solids, compounds **3** are air-stable and can be stored for months without any precautions. In a solution, however, they are prone to gradual oxidation (particularly when exposed to air).

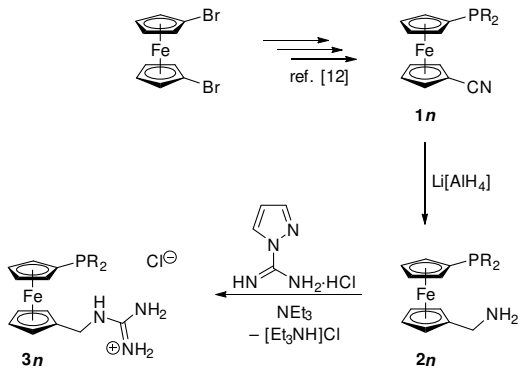

Scheme 2. Synthesis of the ligands **3a**, **3b** and **3d** [R = *i*-Pr (**a**), Cy (**b**), and Fur (**d**)].

In their ^{1}H NMR spectra, compounds **3** displayed four multiplets of the non-equivalent ferrocene protons, a NH-coupled doublet due to the methylene linker ($\delta_H \approx 4$), and the signals of the phosphane substituents. The ^{13}C NMR spectra were also fully consistent with the formulation, showing the expected sets of signals due to the unsymmetrically disubstituted ferrocene moiety (with the resonance due to *C*-CH_2 typically shifted to a lower field, $\delta_C \approx 84$), and the signals due to the methylene linker ($\delta_C \approx 40$) and to the guanidinium carbon atom ($\delta_C \approx 156$). The ^{31}P NMR signals were observed at positions typical for the respective ferrocene phosphanes.[14]

The IR spectra of **3** showed broad bands attributable to the N-H stretching modes above 3000 cm^{-1} and several sharp intense bands due to the combined C-N stretching and N-H deformation vibration modes of the guanidinium unit in the 1600-1660 cm^{-1} range.[15] The formulation of **3** was further corroborated by positive-ion ESI MS spectra, which displayed peaks of the respective guanidinium cations, $[R_2PfcCH_2NHC(NH_2)_2]^+$, and their ferrocenylmethylium fragments,[16] $[R_2PfcCH_2]^+$.

In addition to spectroscopic characterisation, the crystal structures of **3a** and **3d** were determined by single-crystal X-ray diffraction analysis. The molecular structures are shown in Figure 1, and the pertinent structural data are outlined in Table 1.

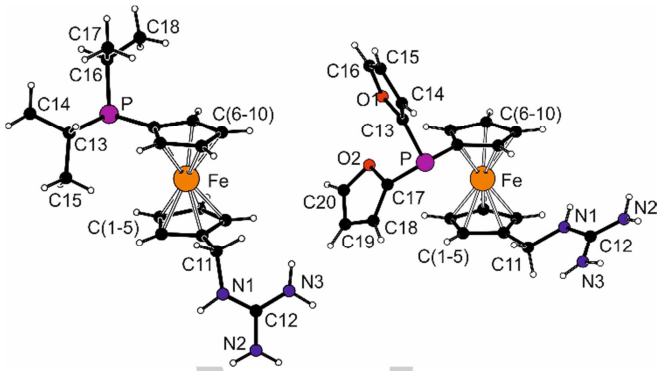

Figure 1. Views of *cations* in the molecular structure of **3a** (left) and **3d** (right). For complete drawings and packing diagrams, see Supporting Information.

Table 1. Selected distances and angles (in Å and deg) for **3a** and **3d**.

Parameter[a]	**3a**	**3d**
Fe-C[b]	2.031(2)-2.066(2)	2.041(2)-2.061(2)
∠Cp1,Cp2	4.8(1)	1.3(1)
τ	–138.7(1)	–80.0(1)
C11-N1	1.472(2)	1.463(2)
C1-C11-N1	111.7(1)	111.8(3)
C12-N1	1.327(2)	1.335(3)
C12-N2	1.343(2)	1.330(3)
C12-N3	1.324(2)	1.326(3)
N-C12-N[c]	118.3(2)-122.8(2)	119.7(2)-120.7(2)
P-C6	1.823(2)	1.810(2)
P-C[R][d]	1.861(2)/1.877(2)	1.815(2)/1.805(2)

[a] Definitions: Cp1 and Cp2 are the planes of the cyclopentadienyl rings C(1-5) and C(6-10), respectively. τ is the torsion angle C1-Cg1-Cg2-C6, wherein Cg1 and Cg2 denote the centroids of the cyclopentadienyl rings Cp1/Cp2. [b] Range of Fe-C(1-10) distances. [c] Range of N1-C12-N2/3 and N2-C12-N3 angles. [d] P-C13/C16 and P-C13/C17 distances for **3a** and **3d**, respectively.

For both compounds, structure determination revealed regular ferrocene moieties with similar Fe-C distances and tilt angles below 5°. The ferrocene cyclopentadienyls were eclipsed in both cases; however, while the substituents in **3a** adopted an approximate 1,3'-conformation, those in **3d** were rotated closer to a 1,2'-conformation. The guanidinium fragments were planar and delocalised, showing similar N-C distances (≈1.33 Å) and N-C-N angles near 120°. The orientation of the guanidinium planes with respect to the plane of the Cp1 ring differed (the dihedral

angles between the guanidine plane and the Cp1 rings were 77.8(1)° in **3a** and 27.1(1)° in **3d**), reflecting intermolecular interactions operating in the crystals. Specifically, the supramolecular structures of both compounds were supported by charge-supported N-H···Cl hydrogen bonds in which the chloride counteranions act as multiple acceptors.[17] When combined, these interactions resulted in the formation of a three-dimensional array in **3a** and in linear H-bonded chains in **3d** (see the Supporting Information).

As functional phosphanes, compounds **3** were used to prepare cationic Rh(I) carbonyl complexes **4** (Scheme 3), which were further catalytically tested (*vide infra*). All complexes were isolated in analytically pure, albeit often solvated, form as air-stable solids. In ^{31}P NMR spectra, they showed one resonance due to the equivalent phosphane moieties, shifted to a lower field with respect to the corresponding free ligand and split into a doublet by interaction with the monoisotopic Rh ($^{1}J_{RhP}$ = 122-132 Hz).[18] In addition, the ^{31}P-coupled ^{13}C{^{1}H} NMR resonances of these phosphane complexes were observed as characteristic apparent triplets arising from virtual coupling within the ^{12}C-^{31}P-^{103}Rh-^{31}P-^{13}C spin systems.[19] The Rh-bound carbonyl ligands were observed as double triplets at low fields (δ_P 184-189) in ^{13}C NMR spectra, while they gave rise to strong characteristic C≡O stretching bands in IR spectra. The energy of these bands symptomatically increased with the decrease in donor ability of the phosphane moiety:[20] ν_{max} 1946 (**4b**) ≈ 1947 (**4a**) < 1970 (**4c**) < 1982 (**4d**) (cm^{-1})

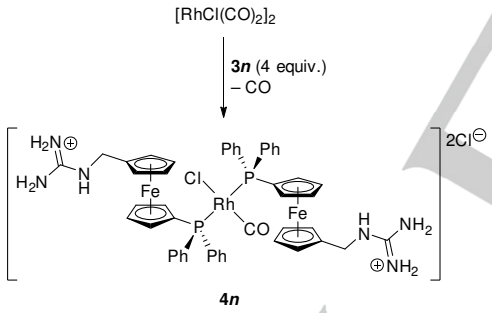

Scheme 3. Synthesis of the Rh(I) complexes **4a-d** [R = *i*-Pr (**a**), Cy (**b**), Ph (**c**), and Fur (**d**)].

Catalytic evaluation

Pd-catalysed cross-coupling reactions. The catalytic properties of the phosphanyl-guanidinium ligands **3** were initially evaluated in Pd-catalysed Suzuki-Miyaura-type C-C cross-coupling between aromatic acyl chlorides and boronic acids producing substituted benzophenones,[21] under reaction conditions adopted from our previous study.[22] In a model reaction (Scheme 4, results in Table 2), *p*-toluoyl chloride reacted with 4-(trifluoromethyl)phenyl boronic acid in the presence of sodium carbonate as a base and 0.1 mol.% of an *in situ*-generated Pd catalyst in a vigorously stirred C_6D_6/water (2 mL each) mixture at 50°C for 1 h to give 4-methyl-4'-(trifluoromethyl)benzophenone. The use of the fluorinated substrate and the deuterated solvent allowed facile reaction monitoring by ^{19}F NMR spectroscopy after adding (trifluoromethyl)benzene as an internal standard.

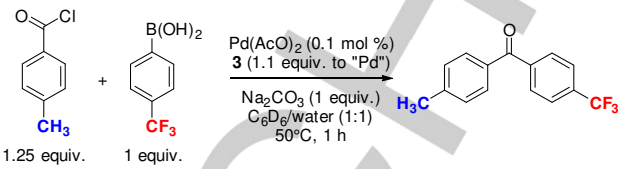

Scheme 4. Pd-catalysed Suzuki-Miyaura cross-coupling of 4-toluoyl chloride with 4-(trifluoromethyl)phenylboronic acid used for screening experiments.

When unsupported $Pd(AcO)_2$ was utilised as the pre-catalyst, palladium black formed almost immediately in the reaction mixture, and conversion reached only ≈30% after 1 hour. In the presence of an auxiliary phosphane ligand (1.1 equiv. with respect to $Pd(OAc)_2$), the formation of palladium black was visibly slower, and conversion increased to ≈85% (Table 2). Although no marked differences between ligands **3** were noted, ligands bearing electron-poor phosphane substituents (**3c** and **3d**) performed better with some test reaction substrates, affording the coupling product in yields higher than their electron-rich counterparts and non-functional phosphanes (including $FcPPh_2$ as an analogue of **3c**).

Table 2. Yields of the coupling product achieved in the model reaction with different in situ formed catalysts.[a]

Catalytic system	NMR Yield	Catalytic system	NMR Yield
$Pd(AcO)_2$	30%	$Pd(AcO)_2$/**3a**	80%
$Pd(AcO)_2/PPh_3$	83%	$Pd(AcO)_2$/**3b**	84%
$Pd(AcO)_2/PCy_3$	85%	$Pd(AcO)_2$/**3c**	93%
$Pd(AcO)_2/FcPPh_2$	86%	$Pd(AcO)_2$/**3d**	95%

[a] For conditions, see the text and Experimental section. The yields were determined by ^{19}F NMR spectroscopy and are an average of two independent runs.

Subsequently, substrates incorporating methyl or trifluoromethyl groups in *para* positions or their unsubstituted (phenyl) analogues were used to compare the influence of the substrate on the yield of the coupling product (Scheme 5). This set of experiments was designed so that the trifluoromethyl group was always present in at least one substrate in order to use the same method of yield determination.

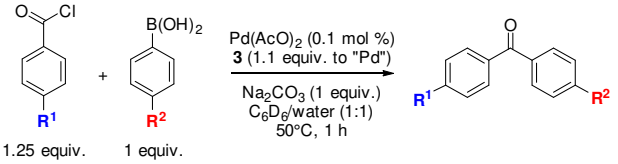

Scheme 5. General depiction of Pd-catalysed Suzuki-Miyaura cross-couplings of aromatic acyl chlorides with arylboronic acids.

While the model reaction used for initial screening was better mediated by Pd catalysts with the weakest donating phosphane ligands of the series (Table 3, entry 1), no such clear trends or significant differences were found in reactions with other substrates. Generally, yields of 65% or higher were achieved with all ligand-substrate combinations. However, in the reaction of substrates with exchanged substituents (entry 2), the best results were found when using electronically dissimilar phosphane ligands **3a** and **3c**. Similar results (albeit with uniformly higher yields) were noted in the coupling of benzoyl chloride with 4-(trifluoromethyl)phenylboronic acid (entry 3). The yields of the complementary reaction between phenylboronic acid and 4-$CF_3C_6H_4C(O)Cl$ (entry 4) were generally lower, with **3b** and **3c** giving the best results. Lastly, when the CF_3 group was present in both substrates, $Pd(OAc)_2$/**3d** catalyst provided the best yield of the coupling product despite rather minor variations between individual Pd-**3** catalysts (6% in absolute figures).

Generally, ligands **3a** and **3d** gave rise to catalysts with the most varying yields, while the Ph_2P-substituted phosphane **3c** proved to be a rather universal ligand for these transformations. As for the substrates, the coupling reaction proceeded better with electron-poor boronic acids. Conversely, relatively worse results were achieved when using electron-poor acyl chlorides, except for coupling reactions in which both reaction components bore electron-withdrawing substituents.

Table 3. Influence of substrate substituents in reactions employing different $Pd(OAc)_2$/**3** catalysts[a]

entry	R^1	R^2	Ligand/NMR yield			
			3a	**3b**	**3c**	**3d**
1	Me	CF_3	80%	84%	93%	95%
2	CF_3	Me	82%	71%	81%	70%
3	H	CF_3	89%	82%	88%	81%
4	CF_3	H	69%	72%	74%	66%
5	CF_3	CF_3	89%	85%	87%	91%

[a] For conditions, see the text and Experimental section. The yields were determined by ^{19}F NMR spectroscopy and represent an average of two independent runs.

The second Pd-mediated transformation investigated was the archetypal Suzuki-Miyaura biaryl coupling of aryl bromides and boronic acids. This reaction was performed under identical reaction conditions, which were quite challenging considering previous reports on similar ligands.[23] Similarly to other experiments, the screening experiments employed a pair of complementary reaction producing 4-methyl-4'-(trifluoromethyl)biphenyl (Scheme 6, R^1/R^2 = Me/CF_3 and CF_3/Me).

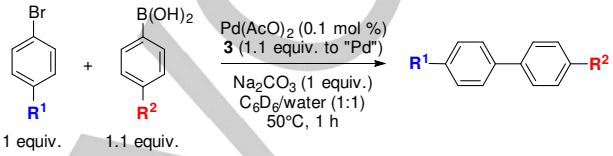

Scheme 6. Pd-catalysed Suzuki-Miyaura cross-coupling of aryl bromides with arylboronic acids.

In the coupling of 4-bromotoluene with 4-(trifluoromethyl)phenylboronic acid (Table 4), unsupported $Pd(AcO)_2$ ensued in a negligible yields, and poor results were also found when using catalysts containing PPh_3 and $FcPPh_2$ as supporting ligands. Of the tested simple phosphanes, the electron-donating alkyl phosphane PCy_3 performed best. Indeed, the catalysts supported by ligands **3** showed similar trends, albeit with considerably increased yields; the most active catalyst resulted from the isopropyl phosphane **3a**.

Notably, the yields of the coupling product increased upon switching substrate substituents (*i.e.*, in the reaction of 4-(trifluromethyl)bromobenzene with 4-tolylboronic acid), except for the poorly active Pd/**3d** catalyst, whose performance remained nearly the same and was thus surpassed even by a catalyst based on $FcPPh_2$. The best results in this reaction were achieved when using the bulky and electron-rich cyclohexyl-substituted ligand **3b**, which resulted in nearly quantitative conversion under the specified conditions.

Table 4. Results from catalytic tests in Suzuki-Miyaura biaryl coupling.[a]

Catalyst	Substrates/NMR Yield	
	R^1 = Me, R^2 = CF_3	R^1 = CF_3, R^2 = Me
$Pd(AcO)_2$	<1%	5%
$Pd(AcO)_2/PPh_3$	6%	25%
$Pd(AcO)_2/PCy_3$	38%	29%
$Pd(AcO)_2/FcPPh_2$	8%	56%
$Pd(AcO)_2$/**3a**	52%	75%
$Pd(AcO)_2$/**3b**	47%	91%

$Pd(AcO)_2$/**3c**	14%	34%
$Pd(AcO)_2$/**3d**	9%	7%

[a] For conditions, see the Experimental section. The yields were determined by ^{19}F NMR spectroscopy and are an average of two independent runs.

Rh-Catalysed hydroformylation. The second type of catalytic reaction was Rh-catalysed hydroformylation of 1-hexene (Scheme 7). The cationic Rh(I)-diphosphane complexes **4a-d** were employed as defined pre-catalysts at a 1-hexene-to-Rh ratio of 400 *without* adding any co-catalyst (free ligand **3** included), and the catalytic reaction was performed under 10 bar of synthesis gas ($CO:H_2$ = 1:1) at 80°C for 5 h. When performing the reaction in neat 1-hexene and in pure toluene or water as solvents (1.5-3.0 mL of solvent per 1.5 mL of 1-hexene), the yields of the aldehydes were disappointingly low (below 10%). Substantially better results were found when using DMSO, mostly likely because the catalysts were more soluble in DMSO (Table 5).

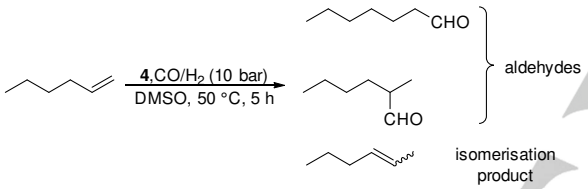

Scheme 7. Rh-catalysed hydroformylation of 1-hexene and the competing isomerisation reaction giving 2-hexene

All catalysts produced heptanals with high selectivity; the fraction of 2-hexene (isomerisation product) was lower than 4% of the amount of aldehydes formed. Complex **4d** bearing the furyl-substituted phosphane ligand led to consistently lowest conversions. This can be explained by the easier dissociation of these weaker-donating phosphane ligands and subsequent catalyst deactivation. However, the selectivity for branched aldehyde (*n*/*iso* ratio) achieved with this catalyst was the highest among all compounds tested, followed by compound **4c**.

Decreasing the amount of the catalyst (Rh:1-hexene = 800 and 1600; see Table 5) expectedly lowered the conversion but had only a minor effect on the selectivity, especially on the *n*/*iso* ratio. The catalytic results remained reproducible even at the lowest catalyst loading. Surprisingly, adding free ligand to the reaction mixture (1 or 2 molar equiv. of **3b** to catalyst **4b**, or 1 molar equiv. of **3c** to catalyst **4c**) adversely affected the catalytic reaction. No pressure drop or products were detected (neither 2-hexene, nor aldehydes), presumably because phosphine ligands compete with olefin and block access to rhodium, thereby inhibiting the reaction.

Table 5. Summary of the hydroformylation results[a]

Catal.	S:Rh[b]	Conv. [%]	2-hexene [%]	Aldehydes [%]	*n*/*iso*
4a	400	95	1	94	1.1
4a	800	92	2	92	1.1
4a	1600	8.4	0.1	8.3	1.4
4b	400	99	1	98	1.1
4b	800	85	1	84	1.1
4b	1600	51	1	50	1.2
4c	400	99	4	95	2.2
4c	800	93	4	89	2.3
4c	1600	47	1	46	2.6
4d	400	59	2	57	2.6
4d	800	53	1.3	52	2.7
4d	1600	43	1	42	2.8

[a] Conditions: 0.75 ml 1-hexene (6 mmol), dimethylsulfoxide (0.75 mL), 10 bar of syngas (H_2/CO = 1:1), 80°C, reaction time: 5 h. [b] 1-hexene:Rh ratio.

Conclusions

In summary, we have demonstrated that our synthetic procedure for the preparation of **3c** can be adapted for the synthesis of analogous ligands (from free amines **2**) bearing different phosphane substituents, which–as the only donor groups available in the ligands in their native state–control the catalytic properties of these compounds. The results from the catalytic tests showed that catalytic activity is determined by a delicate interplay between steric and electronic properties of phosphane substituents, which also influence the overall chemical stability of the catalyst (activation/deactivation and possible formation of metal particles), on the one hand, and the properties of the reaction substrates, on the other. For instance, the reaction outcome of Pd-catalysed cross-coupling reactions mediated by the $Pd(OAc)_2$/**3** system depended not only on the type of reaction (biaryl coupling *vs*. acylative coupling) but also on the substrates (presumably on the electronic influence of the substituents, whose steric influence can be expected to be minimal). In the case of Rh-catalyst hydroformylation using complexes **4** as precatalysts, the phosphane substituents played a minor role (except for the furyl group).

Unsurprisingly, therefore, no universal ligand was identified in the series. While the results showed that the diphenylphosphanyl-substituted compound **3c** was the most practical in "carbonylative" cross-coupling and hydroformylation,

giving rise to reasonably active and stable catalysts, biaryl Suzuki-Miyaura cross-coupling was best mediated by catalysts containing electron-rich alkylphosphane ligands. Conversely, the beneficial effect of the guanidinium pendant was demonstrated for both types of reaction, most likely resulting from enhanced solubility of the catalyst in the polar reaction media.

Experimental Section

Materials and methods

All syntheses were performed under an argon atmosphere using standard Schlenk techniques. Triethylamine was dried over sodium metal and distilled under an argon atmosphere. Other chemicals were purchased from Sigma-Aldrich or Alfa-Aesar (reagent grade) and used without additional purification. Compounds **1a**, **1b**, and **1d**,[12] and **3c**[6] were prepared as previously described. Anhydrous THF and methanol, used during syntheses, were obtained from a Pure Solv MD5 solvent purification system (Innovative Technology, USA). Acetone was dried over potassium carbonate and distilled under an argon atmosphere. Solvents used for workup and for crystallisations were purchased from LachNer (Czech Republic) and used as received. Deuterated solvents were the products of Armar Chemicals and used as obtained. ^{1}H, ^{13}C{^{1}H}, and ^{31}P{^{1}H} NMR spectra were recorded at 25°C on a Varian INOVA 400 spectrometer operating at 399.95, 100.58, and 161.90 MHz, respectively. Chemical shifts (δ in ppm) are given relative to internal tetramethylsilane (^{1}H and ^{13}C) and to external 85% aqueous H_3PO_4 (^{31}P) as an external reference. In addition, ^{19}F NMR spectra used to monitor the catalytic reactions, as well as ^{1}H, ^{13}C and ^{19}F NMR spectra of the catalytic products, were recorded on a Bruker Avance III 400 spectrometer with operating frequencies 400.13, 100.61 and 376.46 MHz using tetramethylsilane (^{1}H and ^{13}C) as an internal reference, and neat trichlorofluoromethane (^{19}F) as an external reference. In addition to the standard description of signal multiplicity,[24] vt and vq were used to distinguish virtual triplets and quartets due to the magnetically non-equivalent protons at the cyclopentadienyl rings (spin systems AA'BB' and AA'BB'X for the methylene- and phosphanyl-substituted rings, respectively, where A, B = ^{1}H, and X = ^{31}P). FTIR spectra were recorded in Nujol mulls on a Nicolet 6700 FTIR spectrometer over the 400–4000 cm^{-1} range. ESI mass spectra were recorded on a Compact QTOF-MS spectrometer (Bruker Daltonics) for samples dissolved in HPLC-grade methanol. Elemental analyses were performed using a Perkin–Elmer 2400 Series II CHNS/O analyser. The presence of residual solvent(s) was confirmed by NMR analysis.

Syntheses

[1'-(Diisopropylphosphanyl)ferrocene-1-yl]methylamine (2a). 1-Cyano-1′-(diisopropylphosphanyl)ferrocene (**1a**; 1.31 g, 4.0 mmol) was dissolved in dry THF (40 mL), and the resulting red solution was transferred dropwise via a cannula into a separate flask containing Li[AlH$_4$] (0.46 g, 12.0 mmol), which was cooled to 0°C in an ice bath. The bubbling turbid mixture was stirred at 0°C for 15 min and then at room temperature for 4 h. Then, the reaction mixture was cooled on ice and quenched by successively adding water (1 mL), 1 M aqueous NaOH (1.5 mL) and additional water (2 mL). The resulting mixture was stirred while cooling for 15 min and then filtered through a short Celite column. The Celite was washed with diethyl ether (3× 10 mL), and the combined organic phases were washed with brine (20 mL) and dried over anhydrous MgSO$_4$. The solvents were evaporated under reduced pressure to give 1.28 g (96%) of **2a** as a viscous orange oil, which was sufficiently pure for further reactions (> 90-95%; the remaining fraction was the residual solvent). An analytical sample was prepared by flash column chromatography (silica gel, dichloromethane/methanol 10:1).

^{1}H NMR (399.95 MHz, CDCl$_3$): δ = 1.07 (dd, $^{3}J_{HH}$ = 6.9 Hz, $^{3}J_{HP}$ = 6.9 Hz, 6 H, CH*Me*$_2$), 1.10 (dd, $^{3}J_{HH}$ = 7.0 Hz, $^{3}J_{HP}$ = 8.7 Hz, 6 H, CH*Me*$_2$), 1.92 (sept of d, $^{3}J_{HH}$ = 7.0 Hz, $^{2}J_{HP}$ = 2.6 Hz, 2 H, C*H*Me$_2$), 3.58 (s, 2 H, C*H*$_2$NH$_2$), 4.10 (vt, *J′* = 1.8 Hz, 2 H, fc), 4.15 (m, 4 H, fc), 4.26 (vt, *J′* = 1.8 Hz, 2 H, fc) ppm. ^{13}C{^{1}H} NMR (100.58 MHz, CDCl$_3$): δ = 19.90 (d, $^{2}J_{CP}$ = 10 Hz, CH*Me*$_2$), 20.13 (d, $^{2}J_{CP}$ = 15 Hz, CH*Me*$_2$), 23.43 (d, $^{1}J_{CP}$ = 11 Hz, *C*HMe$_2$), 41.16 (s, CH$_2$NH$_2$), 68.17 (s, CH of fc), 69.22 (s, CH of fc), 69.81 (d, J_{CP} = 2 Hz, CH of fc), 71.64 (d, J_{CP} = 10 Hz, CH of fc), 76.22 (d, $^{1}J_{CP}$ = 17 Hz, C^{ipso}–P of fc), 91.26 (s, C^{ipso}–CH$_2$ of fc) ppm. ^{31}P{^{1}H} NMR (161.90 MHz, CDCl$_3$): δ = 1.0 (s, P(*i*Pr)$_2$) ppm. FTIR (Nujol): ν_{max} 3366 w, 3091 m, 1571 m, 1401 w, 1363 m, 1302 m, 1243 m, 1232 m, 1194 w, 1156 m, 1027 s, 961 w, 917 w, 882 m, 826 s, 656 m, 634 m, 607 m, 496 s, 479 m cm^{-1}. HRMS (ESI+): *m/z* calc. for $C_{17}H_{27}FeNOP$ ([M + O + H]$^+$) 348.1174, found 348.1174. The compound is rather unstable towards oxidation and, hence, no reliable microanalytical data could be collected.

[1'-(Dicyclohexylphosphanyl)ferrocene-1-yl]methylamine (2b). Starting with 1-cyano-1′-(dicyclohexylphosphanyl)ferrocene (**1b**; 1.43 g, 3.5 mmol) in 50 mL of THF and with Li[AlH$_4$] (0.40 g, 10.5 mmol), the above procedure afforded **2b** (1.38 g, 96%) as an orange solid, which was sufficiently pure for further reactions. An analytical sample was prepared by flash column chromatography over silica gel using a dichloromethane/methanol mixture (20:1 v/v) as the eluent.

^{1}H NMR (399.95 MHz, CDCl$_3$): δ = 1.00-1.36 (m, 10 H, Cy), 1.62-1.84 (m, 10 H, Cy), 1.86-1.96 (m, 4 H, Cy + NH$_2$), 3.58 (s, 2 H, C*H*$_2$NH$_2$), 4.08 (vt, *J′* = 1.8 Hz, 2 H, fc), 4.12 (vq, *J′* = 1.6 Hz, 2 H, fc), 4.13 (vt, *J′* = 1.7 Hz, 2 H, fc), 4.25 (vt, *J′* = 1.8 Hz, 2 H, fc) ppm. ^{13}C{^{1}H} NMR (100.58 MHz, CDCl$_3$): δ = 26.43 (d, J_{CP} = 1 Hz, Cy), 27.33 (d, J_{CP} = 8 Hz, Cy), 27.41 (d, J_{CP} = 11 Hz, Cy), 30.25 (d, J_{CP} = 13 Hz, Cy), 30.30 (d, J_{CP} = 10 Hz, Cy), 33.51 (d, J_{CP} = 11 Hz, Cy), 41.10 (s, CH$_2$NH$_2$), 68.21 (s, CH of fc), 69.22 (s, CH of fc), 69.79 (d, J_{CP} = 3 Hz, CH of fc), 71.87 (d, J_{CP} = 11 Hz, CH of fc), 76.57 (d, $^{1}J_{CP}$ = 16 Hz, C^{ipso}–P of fc), 90.92 (s, C^{ipso}–CH$_2$ of fc) ppm. ^{31}P{^{1}H} NMR (161.90 MHz, CDCl$_3$): δ = –7.2 (s, PCy$_2$) ppm. FTIR (Nujol): ν_{max} 3369 w, 3282 w, 3096 m, 3087 m, 2726 w, 2665 w, 1634 w, 1606 m, 1552 m, 1401 w, 1344 m, 1328 m, 1306 m, 1272 w, 1262 m, 1231 m, 1191 m, 1174 w, 1166 w, 1154 m, 1110 w, 1053 w, 1034 s, 1028 sh, 1001 m, 938 w, 913 w, 884 m, 866 s, 858 sh, 848s, 826 s, 745 w, 716 m, 629 w, 602 w, 515 s, 496 s, 474 s, 442 m, 423 w cm^{-1}. HRMS (ESI+): *m/z* calc. for $C_{23}H_{35}FeNP$ ([M + H]$^+$) 412.1857, found 412.1851. Anal. Calc. for $C_{23}H_{34}FeNP$ (411.4): C 67.16, H 8.33, N 3.41%. Found: C 66.34, H 8.35, N 3.24%. The compound is hygroscopic and tenaciously retains residual water.

[1'-(Di(2-furyl)phosphanyl)ferrocene-1-yl]methylamine (2d). Starting with 1-cyano-1′-(di(2-furyl)phosphanyl)ferrocene (**1d**; 1.51 g, 4.0 mmol), the same procedure furnished analytically pure **2d** (1.27 g, 84%) as an orange solid, which was sufficiently pure for further reactions.

^{1}H NMR (399.95 MHz, DMSO-d$_6$): δ = 3.24 (s, 2 H, CH$_2$NH$_2$), 3.85 (vt, *J′* = 1.8 Hz, 2 H, fc), 4.03 (vt, *J′* = 1.8 Hz, 2 H, fc), 4.35 (vq, *J′* = 1.9 Hz, 2 H, fc), 4.38 (vt of d, *J′* = 1.9 Hz, *J′* = 0.7 Hz, 2 H, fc), 6.51 (dt, *J* = 3.2 Hz, *J* = 1.7 Hz, 2 H, Fur), 6.76 (ddd, *J* = 3.3 Hz, *J* = 2.0 Hz, *J* = 0.7 Hz, 2 H, Fur), 7.90 (m, 2 H, Fur) ppm. ^{13}C{^{1}H} NMR (100.58 MHz, DMSO-d$_6$): δ = 40.20 (s, CH$_2$NH$_2$), 67.99 (s, 2× CH of fc), 71.25 (d, J_{CP} = 5 Hz, CH of fc), 71.89 (d, $^{1}J_{CP}$ = 6 Hz, C^{ipso}–P of fc), 73.62 (d, J_{CP} = 18 Hz, CH of fc), 92.58 (s, C^{ipso}–CH$_2$ of fc), 110.75 (d, J_{CP} = 6 Hz, CH of Fur), 119.88 (d, J_{CP} = 25 Hz, CH of Fur), 147.31 (d, J_{CP} = 2 Hz, CH of Fur), 151.66 (d, $^{1}J_{CP}$ = 10 Hz, C^{ipso} of Fur) ppm. ^{31}P{^{1}H} NMR (161.90 MHz, DMSO-d$_6$): δ = –65.4 (s, PFur$_2$) ppm. FTIR (Nujol): ν_{max} 3377 m, 3108 m, 3067 m, 2607 w, 1737 w,

1580 m, 1549 m, 1403 m, 1309 w, 1215 w, 1204 w, 1195 m, 1160 m, 1148 s, 1116 s, 1062 m, 1025 s, 1015 s, 1003 s, 978 m, 919 w, 903 m, 883 m, 873 m, 860 s, 836 s, 819 s, 747 vs, 668 sh, 659 m, 646 m, 623 w, 595 m, 523 w, 474 vs, 431 w cm^{-1}. HRMS (ESI+): *m/z* calc. for $C_{19}H_{19}FeNO_2P$ ($[M + H]^+$) 380.0503, found 380.0490. Anal. Calc. for $C_{19}H_{18}FeNO_2P$ (379.2): C 60.19, H 4.79, N 3.69%. Found: C 60.09, H 4.81, N 3.50%.

***N*-{[1'-(diisopropylphosphanyl)ferrocene-1-yl]methyl}guanidine hydrochloride (3a).** A solution of amine **1a** (1.26 g, 3.8 mmol) in dry THF (100 mL) was transferred via a cannula onto solid 1*H*-pyrazole-1-carboxamidine hydrochloride (0.61 g, 4.2 mmol), forming an orange suspension. Dry triethylamine (0.62 mL, 4.4 mmol) was added, and the reaction mixture was stirred in the dark overnight. Then, the orange suspension was diluted with methanol (10 mL), which dissolved all solids, and the reaction mixture turned red. The solution was evaporated, and the red oily crude product was purified by chromatography over a silica gel column with dichloromethane/methanol (10:1). The first two minor bands containing impurities were discarded, and the following major orange band was collected and evaporated. The resulting red viscous product was further crystallized from a hot chloroform/hexane mixture yielding 1.01 g (65%) of **3a** as a dark orange crystalline solid. Crystals suitable for structure determination were obtained by liquid phase diffusion of hexane into a saturated chloroform solution of the compound.

^{1}H NMR (399.95 MHz, DMSO-d_6): δ = 1.00 (dd, $^3J_{HH}$ = 6.8 Hz, $^3J_{HP}$ = 5.0 Hz, 6 H, CH*Me*$_2$), 1.03 (dd, $^3J_{HH}$ = 6.8 Hz, $^3J_{HP}$ = 7.0 Hz, 6 H, CH*Me*$_2$), 1.87 (sept of d, $^3J_{HH}$ = 7.0 Hz, $^2J_{HP}$ = 2.0 Hz, 2 H, C*H*Me$_2$), 4.09 (vt, *J'* = 1.8 Hz, 2 H, fc), 4.09 (d, $^3J_{HH}$ = 5.3 Hz, 2 H, C*H*$_2$NH), 4.20 (vq, *J'* = 1.6 Hz, 2 H, fc), 4.25 (vt, *J'* = 1.8 Hz, 2 H, fc), 4.39 (vt, *J'* = 1.8 Hz, 2 H, fc), 7.32 (very broad s, 4 H, NH_2 of guanidinium), 7.85 (t, $^3J_{HH}$ = 5.3 Hz, 1 H, CH$_2$N*H*) ppm. ^{13}C{^{1}H} NMR (100.58 MHz, DMSO-d_6): δ = 19.69 (d, $^2J_{CP}$ = 11 Hz, CH*Me*$_2$), 19.99 (d, $^2J_{CP}$ = 16 Hz, CH*Me*$_2$), 22.83 (d, $^1J_{CP}$ = 13 Hz, *C*HMe$_2$), 40.02 (s, CH_2NH), 68.89 (s, CH of fc), 69.57 (s, CH of fc), 70.40 (d, J_{CP} = 2 Hz, CH of fc), 71.56 (d, J_{CP} = 10 Hz, CH of fc), 76.24 (d, $^1J_{CP}$ = 20 Hz, C^{ipso}–P of fc), 83.71 (s, C^{ipso}–CH$_2$ of fc), 156.65 (s, C^{ipso} of guanidinium) ppm. ^{31}P{^{1}H} NMR (161.90 MHz, DMSO-d_6): δ = –0.6 (s, P(*i*Pr)$_2$) ppm. FTIR (Nujol): ν_{max} 3454 m, 3284 m, 3215 m, 3090 s, 1663 s, 1640 s, 1611 s, 1359 m, 1340 m, 1299 w, 1234 m, 1195 w, 1155 m, 1100 w, 1039 m, 1017 w, 925 w, 884 w, 841 w, 830 m, 816 w, 753 m, 724 w, 655 w, 636 m, 607 m, 585 w, 533 m, 518 w, 501 m, 478 m cm^{-1}. MS (ESI+): *m/z* 315 ([*i*Pr$_2$PfcCH$_2$]$^+$), 374 ([*i*Pr$_2$PfcCH$_2$NHC(NH$_2$)$_2$]$^+$). Anal. Calc. for $C_{18}H_{29}ClFeN_3P$ (409.7): C 52.77, H 7.13, N 10.26%. Found: C 52.45, H 7.18, N 10.04%.

***N*-{[1'-(dicyclohexylphosphanyl)ferrocene-1-yl]methyl}guanidine hydrochloride (3b).** A solution of amine **2b** (1.65 g, 4.0 mmol) in dry THF (100 mL) was transferred via a cannula onto solid 1*H*-pyrazole-1-carboxamidine hydrochloride (0.65 g, 4.4 mmol), producing a yellow suspension. Dry triethylamine (0.62 mL, 4.4 mmol) was introduced, and the resulting mixture was stirred in the dark overnight. On the following day, the turbid orange mixture was concentrated under vacuum, forming an orange oil as the crude product, which was purified by chromatography over a silica gel column using dichloromethane/methanol (5:1) as the eluent. The first minor bands containing impurities and/or side products were discarded, and the following major orange band was collected. Evaporation led to an orange oil, which was further crystallized from a hot chloroform/hexane mixture to give 1.53 g (78%) of **3b** as a yellow microcrystalline powder.

^{1}H NMR (399.95 MHz, DMSO-d_6): δ = 0.90-1.34 (m, 10 H, Cy), 1.57-1.78 (m, 10 H, Cy), 1.82-1.92 (m, 2 H, Cy), 4.07 (vt, *J'* = 1.8 Hz, 2 H, fc), 4.08 (d, $^3J_{HH}$ = 4.2 Hz, 2 H, C*H*$_2$NH), 4.16 (vq, *J'* = 1.6 Hz, 2 H, fc), 4.23 (vt, *J'* = 1.8 Hz, 2 H, fc), 4.38 (vt, *J'* = 1.8 Hz, 2 H, fc), 7.31 (very broad s, 4 H, NH_2 of guanidinium), 7.81 (s, 1 H, CH$_2$N*H*) ppm. ^{13}C{^{1}H} NMR (100.58 MHz, DMSO-d_6): δ = 26.04 (s, Cy), 26.62 (d, J_{CP} = 9 Hz, Cy), 26.77 (d, J_{CP} = 11 Hz, Cy), 29.74 (d, J_{CP} = 10 Hz, Cy), 29.76 (d, J_{CP} = 13 Hz, Cy), 32.89 (d, J_{CP} = 13 Hz, Cy), 40.03 (s, CH_2NH), 68.90 (s, CH of fc), 69.54 (s, CH of fc), 70.38 (d, J_{CP} = 2 Hz, CH of fc), 71.77 (d, J_{CP} = 11 Hz, CH of fc), 76.59 (d, $^1J_{CP}$ = 19 Hz, C^{ipso}–P of fc), 83.66 (s, C^{ipso}–CH$_2$ of fc), 156.60 (s, C^{ipso} of guanidinium) ppm. ^{31}P{^{1}H} NMR (161.90 MHz, DMSO-d_6): δ = –9.3 (s, PCy$_2$) ppm. FTIR (Nujol): ν_{max} 3331 s, 3253 s, 3136 s, 2667 w, 1660 s, 1644 s, 1608 s, 1558 w, 1411 m, 1341 m, 1262 w, 1239 w, 1199 m, 1176 w, 1156 m, 1109 w, 1083 w, 1039 m, 1029 m, 1000 w, 845 m, 838 m, 819 w, 722 w, 663 m, 630 w, 581 m, 530 w, 505 m, 493 m, 473 m cm^{-1}. Anal. Calc. for $C_{24}H_{37}ClFeN_3P$ (489.8): C 58.85, H 7.61, N 8.58%. Found: C 58.73, H 7.50, N 8.51%. MS (ESI+): *m/z* 395 ([Cy$_2$PfcCH$_2$]$^+$), 454 ([Cy$_2$PfcCH$_2$NHC(NH$_2$)$_2$]$^+$).

***N*-{[1'-(di(2-furyl)phosphanyl)ferrocene-1-yl]methyl}guanidine hydrochloride (3d).** A solution of amine **2d** (1.27 g, 3.4 mmol) in dry THF (80 mL) was transferred via a cannula onto 1*H*-pyrazole-1-carboxamidine hydrochloride (0.54 g, 3.7 mmol), giving rise to an orange suspension. After adding dry triethylamine (0.50 mL, 3.7 mmol), the reaction mixture was stirred ,in the dark overnight. On the following day, the orange solution was evaporated and the resulting dark orange oil was subjected to chromatography over a silica gel column using dichloromethane/methanol (10:1) as the eluent. After removing the first yellow band, due to side products, the polarity of the eluent was replaced with dichloromethane/methanol (5:1) to elute the major orange band due to the product. Subsequent evaporation produced **3d** as a sticky orange foam, which was further crystallized from a hot ethanol/diethyl ether mixture to give 1.18 g (76%) of analytically pure **3d** as orange crystals (plates). Crystals used for structure determination were grown by liquid-phase diffusion of methyl *tert*-butyl ether into a methanol solution.

^{1}H NMR (399.95 MHz, DMSO-d_6): δ = 3.92 (vt, *J'* = 1.9 Hz, 2 H, fc), 3.96 (d, $^3J_{HH}$ = 5.7 Hz, 2 H, C*H*$_2$NH), 4.11 (vt, *J'* = 1.9 Hz, 2 H, fc), 4.44 (vq, *J'* = 1.9 Hz, 2 H, fc), 4.47 (vt of d, *J'* = 1.8 Hz, *J'* = 0.7 Hz, 2 H, fc), 6.52 (dt, *J* = 3.3 Hz, *J* = 1.7 Hz, 2 H, Fur), 6.79 (ddd, *J* = 3.3 Hz, *J* = 2.0 Hz, *J* = 0.8 Hz, 2 H, Fur), 7.28 (very broad s, 4 H, NH_2 of guanidinium), 7.80 (t, $^3J_{HH}$ = 5.7 Hz, 1 H, CH$_2$N*H*), 7.92 (m, 2 H, Fur) ppm. ^{13}C{^{1}H} NMR (100.58 MHz, DMSO-d_6): δ = 39.67 (s, CH_2NH), 68.89 (s, CH of fc), 68.98 (s, CH of fc), 71.84 (d, J_{CP} = 5 Hz, CH of fc), 72.59 (d, $^1J_{CP}$ = 5 Hz, C^{ipso}–P of fc), 74.10 (d, J_{CP} = 18 Hz, CH of fc), 84.48 (s, C^{ipso}–CH$_2$ of fc), 110.81 (d, J_{CP} = 6 Hz, CH of Fur), 120.02 (d, J_{CP} = 25 Hz, CH of Fur), 147.44 (d, J_{CP} = 2 Hz, CH of Fur), 151.47 (d, J_{CP} = 10 Hz, C^{ipso} of Fur), 156.60 (s, C^{ipso} of guanidinium) ppm. ^{31}P{^{1}H} NMR (161.90 MHz, DMSO-d_6): δ = –65.9 (s, PFur$_2$) ppm. FTIR (Nujol): ν_{max} 3454 s, 3239 s, 3124 s, 3077 sh, 2725 w, 1664 s, 1640 s, 1603 s, 1552 w, 1424 w, 1332 w, 1309 w, 1260 w, 1203 w, 1196 w, 1164 m, 1148 m, 1115 m, 1063 w, 1038 m, 1029 m, 1005 s, 986 w, 933 w, 900 m, 880 w, 838 m, 832 sh, 822 m, 759 w, 747 s, 721 w, 661 w, 650 m, 594 m, 568 m, 536 w, 509 w, 487 m, 474 s, 459 m cm^{-1}. MS (ESI+): *m/z* 363 ([Fur$_2$PfcCH$_2$]$^+$), 422 ([Fur$_2$PfcCH$_2$NHC(NH$_2$)$_2$]$^+$). Anal. Calc. for $C_{20}H_{21}ClFeN_3O_2P$ (457.7): C 52.49, H 4.63, N 9.18%. Found: C 52.35, H 4.70, N 9.02%.

General procedure for the preparation of complexes [RhCl(CO){R$_2$PfcCH$_2$NHC(NH$_2$)$_2$-κ*P*}$_2$]Cl$_2$ (4). Dry methanol (5 mL) was added atmosphere to the mixture of [Rh(μ-Cl)(CO)$_2$]$_2$ (29.2 mg, 0.075 mmol) and respective ligand (0.300 mmol). The educts dissolved with gas evolution, producing an orange solution, which was stirred at room temperature for 60 minutes. The solvent was evaporated under reduced pressure, leaving amorphous orange solid, which was triturated with acetone. The precipitated product was filtered off, washed with pentane and dried over sodium hydroxide under vacuum. The yield of the product typically exceeds 90%.

Analytical data for 4a. Yellow solid. ^{1}H NMR (399.95 MHz, DMSO-d_6): δ = 1.22 (d of vt, $J_1 \approx J_2 \approx 7.3$ Hz, 12 H, CH*Me*$_2$), 1.35 (d of vt, $J_1 \approx J_2 \approx 7.5$ Hz, 12 H, CH*Me*$_2$), 2.74 (m, 4 H, C*H*Me$_2$), 4.14 (d, $^{3}J_{HH}$ = 5.2 Hz, 4 H, C*H*$_2$NH), 4.35 (vt, *J'* = 1.8 Hz, 4 H, fc), 4.37 (vt, *J'* = 1.8 Hz, 4 H, fc), 4.56 (vt, *J'* = 1.8 Hz, 4 H, fc), 4.67 (vt, *J'* = 1.7 Hz, 4 H, fc), 7.32 (br s, 8 H, NH$_2$ of guanidinium), 7.88 (s, 2 H, CH$_2$N*H*) ppm. ^{13}C{^{1}H} NMR (100.58 MHz, DMSO-d_6): δ = 18.65 (s, CH*Me*), 20.02 (s, CH*Me*), 25.47 (vt, *J'* = 13 Hz, *C*HMe), 39.87 (s, CH$_2$NH), 69.30 (s, CH of fc), 70.70 (s, CH of fc), 71.30 (vt, *J'* = 3 Hz, s, CH of fc), 73.73 (vt, *J'* = 5 Hz, s, CH of fc), 74.64 (vt, *J'* = 19 Hz, s, C^{ipso}–P of fc), 84.44 (s, C^{ipso}–CH$_2$ of fc), 156.67 (s, C^{ipso} of guanidinium), 188.37 (dt, $^{1}J_{RhC}$ = 74 Hz, $^{2}J_{PC}$ = 16 Hz, C≡O) ppm. ^{31}P{^{1}H} NMR (161.90 MHz, DMSO-d_6): δ = 38.2 (d, $^{1}J_{RhP}$ = 122 Hz, P(*i*Pr)$_2$) ppm. FTIR (Nujol): ν_{max} 3319 m, 3245 m, 3134 s, 1947 s, 1935 sh, 1707 w, 1663 s, 1653 s, 1341 w, 1305 w, 1252 w, 1226 w, 1195 w, 1161 m, 1092 w, 1041 sh, 1030 m, 928 w, 885 w, 834 m, 820 w, 665 m, 629 m, 616 w, 603 w, 580 m, 545 w, 535 w, 485 m cm^{-1}. MS (ESI+): *m/z* 293 ([M – 3Cl]$^{3+}$), 439 ([M – 2Cl – HCl]$^{2+}$), 877 ([M – Cl – 2HCl]$^{+}$), 913 ([M – Cl – HCl]$^{+}$). Anal. Calcd. for $C_{37}H_{58}Cl_3Fe_2N_6OP_2Rh \cdot ½Me_2CO \cdot ½H_2O$ (1023.9): C 45.17, H 6.10, N 8.21%. Found C 44.93, H 5.77, N 8.00%.

Analytical data for 4b. Yellow solid. ^{1}H NMR (399.95 MHz, DMSO-d_6): δ = 1.06-1.34 (m, 12 H, Cy), 1.40-1.55 (m, 8 H, Cy), 1.60-1.69 (m, 4 H, Cy), 1.70-1.82 (m, 8 H, Cy), 1.93-2.03 (m, 4 H, Cy), 2.16-2.27 (m, 4 H, Cy), 2.41-2.52 (m, 4 H, Cy), 4.13 (d, $^{3}J_{HH}$ = 5.6 Hz, 4 H, C*H*$_2$NH), 4.30 (vt, *J'* = 1.8 Hz, 4 H, fc), 4.35 (vt, *J'* = 1.8 Hz, 4 H, fc), 4.55 (vt, *J'* = 1.7 Hz, 4 H, fc), 4.62 (m, 4 H, fc), 7.10 (br s, 4 H, NH$_2$ of guanidinium), 7.52 (br s, 4 H, NH$_2$ of guanidinium), 7.84 (t, $^{3}J_{HH}$ = 5.4 Hz, 2 H, CH$_2$N*H*) ppm. ^{13}C{^{1}H} NMR (100.58 MHz, DMSO-d_6): δ = 25.90 (s, Cy), 26.80 (two vt, 2× Cy), 28.44 (s, Cy), 29.55 (s, Cy), 35.86 (vt, *J'* = 12 Hz, Cy), 69.38 (s, CH of fc), 70.62 (s, CH of fc), 71.26 (s, CH of fc), 74.15 (vt, *J'* = 5 Hz, CH of fc), 74.29 (vt, *J'* = 19 Hz, C^{ipso}–P of fc), 84.46 (s, C^{ipso}–CH$_2$ of fc), 156.63 (s, C^{ipso} of guanidinium), 188.78 (dt, $^{1}J_{RhC}$ = 74 Hz, $^{2}J_{PC}$ = 16 Hz, C≡O) ppm. The signal due to the methylene spacer overlaps with the solvent resonance. ^{31}P{^{1}H} NMR (161.90 MHz, DMSO-d_6): δ = 29.8 (d, $^{1}J_{RhP}$ = 122 Hz, PCy$_2$) ppm. FTIR (Nujol): ν_{max} 3326 m, 3158 m, 1946 s, 1939 sh, 1665 s, 1645 s, 1342 w, 1328 w, 1306 w, 1291 w, 1266 w, 1195 w, 1172 w, 1162 m, 1034 m, 1007 w, 854 w, 848 w, 825 m, 747 m, 625 w, 578 m, 481 m, 467 m cm^{-1}. MS (ESI+): *m/z* 346 ([M – 3Cl]$^{3+}$), 519 ([M – 2Cl – HCl]$^{2+}$), 1037 ([M – Cl –2HCl]$^{+}$), 1073 ([M – Cl – HCl]$^{+}$). Anal. Calc. for $C_{49}H_{74}Cl_3Fe_2N_6OP_2Rh \cdot H_2O$ (1164.1): C 50.56, H 6.58, N 7.22%. Found C 50.31, H 6.42, N 6.99%.

Analytical data for 4c. Yellow solid. ^{1}H NMR (399.95 MHz, DMSO-d_6): δ = 4.05 (d, $^{3}J_{HH}$ = 5.7 Hz, 4 H, C*H*$_2$NH), 4.38 (vt, *J'* = 1.7 Hz, 4 H, fc), 4.40 (vt, *J'* = 1.7 Hz, 4 H, fc), 4.44 (s, 4 H, fc), 4.62 (vt, *J'* = 1.7 Hz, 4 H, fc), 7.44-7.52 (m, 12 H, Ph), 7.56-7.64 (m, 8 H, Ph), 7.87 (s, 2 H, CH$_2$N*H*). ^{13}C{^{1}H} NMR (100.58 MHz, DMSO-d_6): δ = 69.48 (s, CH of fc), 70.92 (s, CH of fc), 72.60 (vt, *J'* = 2 Hz, CH of fc), 74.33 (vt, *J'* = 26 Hz, C^{ipso}–P of fc), 74.64 (vt, *J'* = 6 Hz, CH of fc), 84.96 (s, C^{ipso}–CH$_2$ of fc), 128.08 (vt, *J'* = 5 Hz, CH of Ph), 130.17 (s, CH of Ph), 133.37 (vt, *J'* = 13 Hz, CH of Ph), 134.34 (vt, *J'* = 23 Hz, C^{ipso} of Ph), 156.66 (s, C^{ipso} of guanidinium), 187.18 (dt, $^{1}J_{RhC}$ = 74 Hz, $^{2}J_{PC}$ = 16 Hz, C≡O) ppm. The signal due to the methylene linker overlaps with the solvent resonance. ^{31}P{^{1}H} NMR (161.90 MHz, DMSO-d_6): δ = 22.6 (d, $^{1}J_{RhP}$ = 126 Hz, PPh$_2$) ppm. FTIR (Nujol): ν_{max} 3316 m, 3141 s, 1970 s, 1647 s, 1435 s, 1339 w, 1306 w, 1164 m, 1097 m, 1071 w, 1028 m, 833 m, 746 m, 695 s, 627 w, 572 m, 535 m, 515 m, 496 s, 471 m cm^{-1}. MS (ESI+): *m/z* 507 ([M – 2Cl – HCl]$^{2+}$), 525 ([M – 2Cl]$^{2+}$). Anal. Calcd. for $C_{49}H_{50}Cl_3Fe_2N_6OP_2Rh \cdot ¼ Me_2CO \cdot H_2O$ (1154.4): C 51.76, H 4.67, N 7.28%. Found C 51.63, H 4.64, N 6.73%.

Analytical data for 4d. Yellow solid. ^{1}H NMR (399.95 MHz, DMSO-d_6): δ = 4.10 (d, $^{3}J_{HH}$ = 5.3 Hz, 4 H, C*H*$_2$NH), 4.33 (s, 4 H, fc), 4.38 (s, 4 H, fc), 4.65 (s, 4 H, fc), 4.69 (s, 4 H, fc), 6.63 (s, 4 H, Fur), 6.90 (d, *J* = 3 Hz, 4 H, Fur), 7.30 (br s, 8 H, NH$_2$ of guanidinium), 7.85 (t, $^{3}J_{HH}$ = 5.3 Hz, 2 H, CH$_2$N*H*), 8.07 (s, 4 H, Fur) ppm. ^{13}C{^{1}H} NMR (100.58 MHz, DMSO-d_6): δ = 69.59 (s, CH of fc), 70.27 (vt, *J'* = 30 Hz, C^{ipso}–P of fc), 70.45 (s, CH of fc), 72.61 (s, CH of fc), 74.58 (vt, *J'* = 6 Hz, CH of fc), 85.14 (s, C^{ipso}–CH$_2$ of fc), 111.04 (s, CH of Fur), 122.10 (vt, *J'* = 16 Hz, CH of Fur), 146.61 (vt, *J'* = 36 Hz, C^{ipso} of Fur), 148.37 (s, CH of Fur), 156.64 (s, C$_{ipso}$ of guanidinium), 184.92 (d, $^{1}J_{RhC} \approx 62$ Hz, C≡O) ppm. The signal due to the methylene spacer is probably obscured by the solvent resonance. ^{31}P{^{1}H} NMR (161.90 MHz, DMSO-d_6): δ = –10.9 (d, $^{1}J_{RhP}$ = 132 Hz, PFur$_2$) ppm. FTIR (Nujol): ν_{max} 3110 s, 1982 s, 1663 s, 1647 s, 1550 w, 1366 m, 1341 w, 1308 w, 1236 w, 1213 w, 1196 w, 1168 m, 1121 m, 1062 w, 1028 w, 1009 s, 907 w, 883 w, 833 w, 750 m, 650 w, 621 w, 593 w, 573 m, 534 m, 489 s, 475 sh cm^{-1}. MS (ESI+): *m/z* 422 ([Fur$_2$PfcCH$_2$NHC(NH$_2$)$_2$]$^{+}$), 438 ([Fur$_2$POfcCH$_2$NHC(NH$_2$)$_2$]$^{+}$), 487 ([M – 2Cl – HCl]$^{2+}$), 505 ([M – 2Cl]$^{2+}$), 973 ([M – Cl – 2HCl]$^{+}$). Anal. Calcd. for $C_{41}H_{42}Cl_3Fe_2N_6O_5P_2Rh \cdot ½Me_2CO \cdot ½H_2O$ (1119.8): C 45.59, H 4.14, N 7.51%. Found C 45.51, H 4.21, N 7.00%.

Pd-catalysed cross-coupling of acyl chlorides with boronic acids. In a typical reaction, a dry Schlenk flask was charged successively with the respective aroyl chloride (1.25 mmol), boronic acid (1.0 mmol), sodium carbonate (1.0 mmol) and ligand (1.1 μmol). An argon atmosphere was established, and the flask was stoppered with a septum. Deuterated benzene (1.8 mL), deaerated water (2.0 mL) and, finally, a 5 mM solution of palladium(II) acetate in deuterated benzene (0.2 mL, 1.0 μmol) were introduced. The resulting mixture was vigorously stirred at 50°C for 60 minutes. After cooling to room temperature, the mixture was diluted with water (5 mL) to dissolve the crystallizing ionic components and (trifluoromethyl)benzene (146.1 mg, 1.0 mmol) was added as an internal standard. Conversions were determined by integration of ^{19}F NMR spectra recorded in filtered benzene phase (PTFE syringe filter, 0.45 μm pore size). Characterisation data of the coupling products are given in Supporting Information.

Pd-catalysed cross-coupling of aryl bromides with boronic acids. In a typical run, a dry Schlenk flask was charged with the appropriate aryl bromide (1.0 mmol), boronic acid (1.1 mmol), sodium carbonate (1.0 mmol) and a ligand (1.1 μmol). An argon atmosphere was established and the flask was sealed with a septum. Deuterated benzene (1.8 mL), deaerated water (2.0 mL) and, finally, 5 mM solution of palladium(II) acetate in deuterated benzene (0.2 mL, 1.0 μmol) were added. The resulting mixture was vigorously stirred at 50°C for 60 minutes. After cooling to room temperature, the mixture was diluted with water (5 mL) to dissolve the crystallizing ionic components and (trifluoromethyl)benzene (146.1 mg, 1.0 mmol) was added as an internal standard. The benzene phase was filtered as described above and analysed by ^{19}F NMR spectroscopy to determine the conversion. Characterisation data of the coupling products are available in Supporting Information.

Hydroformylation experiments. These experiments were performed in in a 50mL stainless steel autoclave equipped with a manometer, a thermostat, a magnetic stirrer and a gas inlet/outlet system. The catalyst was placed in the autoclave and, subsequently, 1-hexene and dimethyl sulfoxide (0.75 mL each) were added under nitrogen atmosphere. The autoclave was closed, flushed three times with hydrogen (5 bar) and, finally, pressurized with syngas (H_2/CO = 1:1) to 10 bar and heated to 80°C for 5 h. When the reaction was finished, the autoclave was cooled to ambient temperature and depressurised. The organic phase was separated from the solid residue by vacuum transfer and analysed by GC (Hewlett-Packard 5890 II) and GC-MS (Hewlett-Packard 5971A).

X-Ray crystallography. Full-sphere diffraction data (θ_{max} = 26° for **3a**, and 27.5° for **3d**; completeness > 99%) were recorded using a Nonius Kappa CCD diffractometer equipped with a Bruker Apex II detector (**3d**),

or a Bruker D8 VENTURE Kappa Duo diffractometer with a PHOTON100 detector (**3a**) at 150(2) K. The data were corrected for absorption using multi-scan methods included in the diffractometer software.

Both structures were solved using direct methods (SHEXLT-2014) and subsequently refined by full-matrix least-squares based on F^2 using SHELXL-2014.[25] Compound **3d** was treated as a two-component, non-merohedral twin (twinning matrix: {–1 0 –0.350; 0 –1 0; 0 0 1}, the refined contributions of the two domains: 79:21). All non-hydrogen atoms were refined with anisotropic displacement parameters. The hydrogen atoms residing on the nitrogen atoms (NH) were located on difference density maps and refined as riding atoms with U_{iso}(H) assigned to 1.2U_{eq} of their pivotal atom. Hydrogen atoms bonded to carbon atoms were placed in their theoretical positions and refined similarly. A recent version of the PLATON program[26] was used to prepare all structural diagrams and to calculate all geometric parameters. The numeric values are rounded to their estimated deviations (ESDs) given to one decimal place. Parameters pertaining to atoms in constrained positions are given without ESDs.

Selected crystallographic data and refinement parameters are given in Supporting Information (Table S1). In addition, CCDC 1955576 (for **3a**) and 1955577 (for **3d**) contain the complete crystallographic data for this paper. These data are available free of charge from the Cambridge Crystallographic Data Centre.

Acknowledgments

This work has been supported by the Grant Agency of Charles University (project no. 130317) and by Charles University Research Centre program (project UNCE/SCI/014).

Keywords: phosphane ligands • ferrocene ligands • hydroformylation • cross-coupling • palladium • rhodium

Entry for the Table of Contents

FULL PAPER

A series of phosphanylferrocene ligands with cationic guanidinium tags and varied phosphane substituents was prepared and tested in Pd-catalysed Suzuki-Myiaura cross-coupling reactions and in Rh-catalysed hydroformylation of 1-hexene. The influence of the phosphane substituents on the catalytic properties is discussed.

Ferrocene ligands

*O. Bárta, I. Císařová,[a] E. Mieczyńska,[a] A. M. Trzeciak, P. Štěpnička**

Page No. – Page No.

Synthesis and catalytic evaluation of phosphanylferrocene ligands with cationic guanidium pendants and varied phosphane substituents

REFERENCES

[1] a) F. Joó, *Aqueous Organometallic Catalysis*, Kluwer, Dordrecht, **2001**, b) *Aqueous-Phase Organometallic Catalysis, 2nd ed.* (Eds. B. Cornils, W. Herrmann), Wiley-VCH, Weinheim, **2004**; c) C.-J. Li, *Chem. Rev.* **2005,** *105*, 3095-3165; d) R. N. Butler, A. G. Coyne, *Chem. Rev.* **2010**, *110*, 6302-6337; (d) K. H. Shaughnessy, *Chem. Rev.* **2009**, *109*, 643-710.

[2] For examples of phosphane ligands with guanidinium tags, see: a) A. Hessler, O. Stelzer, H. Dibowski, K. Worm, F. P. Schmidtchen, *J. Org. Chem.* **1997**, *62*, 2362-2369; b) O. Herd, A. Hessler, M. Hingst, P. Machnitzki, M. Tepper, O. Stelzer, *Catal. Today* **1998**, *42*, 413-420; c) P. Machnitzki, M. Tepper, K. Wenz, O. Stelzer, E. Herdtweck, *J. Organomet. Chem.* **2000**, *602*, 158-169; d) P. Wasserscheid, H. Waffenschmidt, P. Machnitzki, K. W. Kottsieper, O. Stelzer, *Chem. Commun.* **2001**, 451-452; d) H. Dibowski, F. P. Schmidtchen, *Tetrahedron* **1995**, *51*, 2325-2330; e) P. Guerreiro, V. Ratovelomanana-Vidal, J.-P. Genêt, P. Dellis, *Tetrahedron Lett.* **2001**, *42*, 3423-3426.

[3] a) T. Šmejkal, B. Breit, *Angew. Chem. Int. Ed.* **2008**, *47*, 311-315; b) T. Šmejkal, B. Breit, *Angew. Chem. Int. Ed.* **2008**, *47*, 3946-3949; c) L. Diab, T. Šmejkal, J. Geier, B. Breit, *Angew. Chem. Int. Ed.* **2009**, *48*, 8022-8026; d) T. Šmejkal, D. Gribkov, J. Geier, M. Keller, B. Breit, *Chem. Eur. J.* **2010**, *16*, 2470-2478; e) D. Fuchs, G. Rousseau, L. Diab, U. Gellrich, B. Breit, *Angew. Chem. Int. Ed.* **2012**, *51*, 2178-2182.

[4] a) *Ferrocenes: Ligands, Materials and Biomolecules* (Ed.: P. Štěpnička), Wiley, Chichester, **2008**; b) *Ferrocenes: Homogeneous Catalysis, Organic Synthesis, Materials Science* (Eds.: A. Togni, T. Hayashi), VCH, Weinheim, **1995**; c) R. C. J. Atkinson, V. C. Gibson, N. J. Long, *Chem. Soc. Rev.* **2004**, *33*, 313-328; d) R. Gómez Arrayás, J. Adrio, J. C. Carretero, *Angew. Chem. Int. Ed.* **2006**, *45*, 7674-7715.

[5] H. Charvátová, I. Císařová, P. Štěpnička, *Eur. J. Inorg. Chem.* **2017**, 288-296.

[6] O. Bárta, I. Císařová, P. Štěpnička, *Eur. J. Inorg. Chem.* **2017**, 489-495.

[7] A. R. Katritzky, B. V. Rogovoy, *ARKIVOC* **2005**, 49-87.

[8] K. Škoch, I. Císařová, P. Štěpnička, *Organometallics* **2015**, *34*, 1942-1956.

[9] a) A. Bader, E. Lindner, *Coord. Chem. Rev.* **1991**, *108*, 27-110; b) C. S. Slone, D. A. Weinberger, C. A. Mirkin, *Progr. Inorg. Chem.* **1999**, *48*, 233-350; b) P. Braunstein, F. Naud, *Angew. Chem. Int. Ed.* **2001**, *40*, 680-699.

[10] a) N. Miyaura, A. Suzuki, *Chem. Rev.* **1995**, *95*, 2457-2483; b) N. Miyaura, *Top. Curr. Chem.* **2002**, *219*, 11-59; c) N. Miyaura in *Metal-Catalyzed Cross-Coupling Reactions* (Eds.: A. de Meijere, F. Diederich), 2nd ed., Wiley-VCH, Weinheim, **2004**; Vol. 1, chapter 2, pp. 41-123; d) *Palladium-Catalyzed Coupling Reactions* (Ed.: Á. Molnár), Wiley-VCH, Weinheim, **2013**; e) I. Maluenda, O. Navarro, *Molecules* **2015**, *20*, 7528-7557.

[11] *Hydroformylation: Fundamentals, Processes, and Applications in Organic Synthesis* (Eds. A. Börner, R. Franke), Wiley-VCH: Weinheim, **2016**, vols. 1 and 2; b) *Rhodium Catalyzed Hydroformylation* (Eds. P. W. N. M. van Leeuwen, C. Claver), Kluwer: New York, **2002**; c) B. Breit, W. Seiche, *Synthesis* **2001**,1-36.

[12] O. Bárta, I. Císařová, J. Schulz, P. Štěpnička, *New J. Chem.* **2019***, 43,* 11258-11262.

[13] M. S. Bernatowicz, Y. Wu, G. R. Matsueda, *J. Org. Chem.* **1992**, *57*, 2497-2502.

[14] J. Schulz, P. Vosáhlo, F. Uhlík, I. Císařová, P. Štěpnička, *Organometallics* **2017**, *36*, 1828-1841.

[15] a) M. Drozd, *Mater. Sci. Eng. B* **2007**, *136*, 20-28; b) M. Drozd, D. Dudzic, *Spectrochim. Acta, Part A: Mol. Biomol. Spectrosc.* **2013**, *115*, 345-356.

[16] a) W. Henderson, A. G. Oliver, A. J. Downard, *Polyhedron* **1996**, *15*, 1165-1173; b) Yu. S. Nekrasov, R. S. Skazov, A. A. Simenel, L. V. Snegur, I. V. Kachala, *Russ. Chem. Bull.* **2006**, *55*, 1368-1371.

[17] a) J. H. Bryden, *Acta Crystallogr.* **1957**, *10*, 677-680; b) D. J. Haas, D. R. Harris, H. H. Mills, *Acta Crystallogr.* **1965**, *19*, 676-679, c) I. Matulková, H. Solařová, P. Štěpnička, I. Císařová, T. Janda, P. Němec, I. Němec, *Opt. Mater.* **2015**, *42*, 39-46.

[18] For similar complexes, see: a) P. Štěpnička, I. Císařová, *J. Chem. Soc., Dalton Trans.* **1998**, 2807-2811, b) M. Zábranský, I. Císařová, A. M. Trzeciak, W. Alsalahi, P. Štěpnička, *Organometallics* **2019**, *38*, 479-488 and ref. 14.

[19] W. H. Hersh, *J. Chem. Educ.* **1997**, *74*, 1485-1488 and references cited therein.

[20] a) S. Vastag, B. Heil, L. Markó, *J. Mol. Catal.* **1979**, *5*, 189-195; b) A. Roodt, S. Otto, G. Steyl, *Coord. Chem. Rev.* **2003**, *245*, 121-137.

[21] M. Blangetti, H. Rosso, C. Prandi, A. Deagostino, P. Venturello, *Molecules* **2013**, *18*, 1188-1213.

[22] H. Solařová, I. Císařová, P. Štěpnička, *Organometallics* **2014**, *33*, 4131-4147.

[23] a) J. Kühnert, M. Dušek, J. Demel, H. Lang, P. Štěpnička, *Dalton Trans.* **2007**, 2802-2811; b) P. Štěpnička, M. Lamač, I. Císařová, *Polyhedron* **2004**, *23*, 921-928; c) J. Tauchman, I. Císařová, P. Štěpnička, *Organometallics* **2009**, *28*, 3288-3302; d) P. Štěpnička, J. Schulz, T. Klemann, U. Siemeling, I. Císařová, *Organometallics* **2010**, *29*, 3187-3200; e) P. Štěpnička, B. Schneiderová, J. Schulz, I. Císařová, *Organometallics* **2013**, *32*, 5754-5765.

[24] R. M. Silverstein, F. X. Webster, D. J. Kiemle, *Spectrometric Identification of Organic Compounds*, 7th ed., Wiley, Hoboken, **2005**.

[25] G. M. Sheldrick, *Acta Crystallogr., Sect. C, Struct. Chem.* **2015**. *71*, 3-8.

[26] A. L. Spek, *J. Appl. Crystallogr.* **2003**, *36*, 7-13.